Sources of carbonaceous aerosols over the United States and implications for natural visibility

Rokjin J. Park and Daniel J. Jacob

Division of Engineering and Applied Sciences, Department of Earth and Planetary Sciences, Harvard University, Cambridge, Massachusetts, USA

Mian Chin

School of Earth and Atmospheric Sciences, Georgia Institute of Technology, Atlanta, Georgia, USA

Randall V. Martin[1]

Division of Engineering and Applied Sciences, Department of Earth and Planetary Sciences, Harvard University, Cambridge, Massachusetts, USA

Received 18 November 2002; revised 29 January 2003; accepted 12 March 2003; published 20 June 2003.

[1] We use a global three-dimensional model (GEOS-CHEM) to better quantify the sources of elemental carbon (EC) and organic carbon (OC) aerosols in the United States through simulation of year-round observations for 1998 at a network of 45 sites (Interagency Monitoring of Protected Visual Environments (IMPROVE)). Simulation with our best a priori understanding of sources, including global satellite data to constrain fire emissions, captures most of the variance in the observations (R^2 = 0.84 for EC, 0.67 for OC) with a low bias of 15% for EC and 26% for OC. Multiple linear regression to fit the IMPROVE data yields best estimates of 1998 U.S. sources of 0.60 Tg year^{-1} EC and 0.52 Tg year^{-1} OC from fossil fuel; 0.07 Tg year^{-1} EC and 0.89 Tg year^{-1} OC from biofuel; 0.08 Tg year^{-1} EC and 0.60 Tg year^{-1} OC from wildfires; and 1.10 Tg year^{-1} OC from vegetation. We find that fires in Mexico and Canada contributed 40–70% of annual mean natural EC in the United States for 1998 and 20–30% of annual mean natural OC. Transpacific transport from Asian pollution sources amounted to less than 10% of the natural EC and less than 2% of the natural OC; in contrast to ozone, we find that intercontinental transport of anthropogenic carbonaceous aerosols does not enhance significantly the natural background. IMPROVE observations and model simulations for the summer of 1995 show that Canadian fire emissions can produce large events of elevated EC and OC in the southeastern United States. Our best estimates of mean natural concentrations of EC and OC in the United States, using a model simulation with climatological monthly mean fire emissions, are 2–3 times higher than the default values recommended by the U.S. Environmental Protection Agency for visibility calculations, except for OC in the eastern United States (16% lower). *INDEX TERMS:* 0305 Atmospheric Composition and Structure: Aerosols and particles (0345, 4801); 0345 Atmospheric Composition and Structure: Pollution—urban and regional (0305); 4801 Oceanography: Biological and Chemical: Aerosols (0305); *KEYWORDS:* carbonaceous aerosols, natural visibility, natural aerosol concentrations, trans-Pacific transport of aerosol, transboundary transport of aerosol, biomass burning aerosol

Citation: Park, R. J., D. J. Jacob, M. Chin, and R. V. Martin, Sources of carbonaceous aerosols over the United States and implications for natural visibility, *J. Geophys. Res.*, *108*(D12), 4355, doi:10.1029/2002JD003190, 2003.

1. Introduction

[2] Carbonaceous aerosol is one of the least understood components of fine particulate matter (PM). It is usually divided in two fractions, elemental carbon (EC) and organic carbon (OC). OC is the second most abundant component of the aerosol in the United States after sulfate, and the dominant component of the natural continental aerosol [*Malm et al.*, 2000]. EC is the dominant component of the light-absorbing aerosol. Carbonaceous aerosol is presently the subject of intense scrutiny because of its impact on human health, visibility, and climate.

[3] We present here an assessment of the sources of EC and OC in the United States by using a global 3-D model (GEOS-CHEM) simulation of observations from the Interagency Monitoring of Protected Visual Environments (IMPROVE) network. Our focus is on quantifying the

[1]Now at Harvard-Smithsonian Center for Astrophysics, Cambridge, Massachusetts, USA.

Copyright 2003 by the American Geophysical Union.
0148-0227/03/2002JD003190

anthropogenic and natural sources of these aerosols, the role of transboundary transport, and the implications for visibility. The U.S. Environmental Protection Agency regional haze rule [*Environmental Protection Agency* (*EPA*), 2001] mandates a schedule of increasing emission controls to achieve "natural visibility conditions" in national parks and other wilderness areas by 2064. The ambiguity in defining "natural visibility conditions" requires better information on natural PM concentrations and the perturbing effects from fires and from sources outside the United States.

[4] Elemental carbon is emitted to the atmosphere by combustion. Major sources in the United States include coal burning and diesel engines. Organic carbon is emitted directly to the atmosphere (primary OC) and formed in situ by condensation of low-volatility products of the photooxidation of hydrocarbons (secondary OC). Primary sources of OC in the United States are wood fuel, coal burning, and wild fires [*Seinfeld and Pandis*, 1998; *Cabada et al.*, 2002]. Secondary OC includes an anthropogenic component from oxidation of aromatic hydrocarbons, and a biogenic component from oxidation of terpenes [*Griffin et al.*, 1999].

[5] Our approach is to conduct a 3-D model simulation of EC and OC concentrations in the United States for 1998, with best a priori sources, compare results with observations from the IMPROVE network, and use the constraints from the comparison to optimize our treatment of sources by multiple linear regression. Our treatment of fire emissions accounts for year-to-year variability through satellite observations; 1998 was a particularly active fire year, thus offering good constraints on emissions from that source. We also present a case study for the summer of 1995 to demonstrate the large-scale enhancements of EC and OC concentrations in the United States that can arise from Canadian fires. We go on to quantify mean natural EC and OC concentrations in the United States for different seasons and regions, using climatological fire emissions and sources from vegetation, and to assess the enhancement of EC and OC background concentrations resulting from transpacific transport of Asian pollution.

2. Model Description

2.1. General

[6] We use the GEOS-CHEM global 3-D model of tropospheric chemistry [*Bey et al.*, 2001] to simulate EC and OC aerosols for 1998 (1 year) and 1995 (summer). The model (version 4.23; see http://www-as.harvard.edu/chemistry/trop/geos/index.html) uses assimilated meteorological data from the NASA Goddard Earth Observing System (GEOS) including winds, convective mass fluxes, mixed layer depths, temperature, precipitation, and surface properties. Meteorological data for 1995 and 1998 are available with 6-hour temporal resolution (3-hour for surface variables and mixing depths), 2° latitude by 2.5° longitude horizontal resolution, and 20 (GEOS1 for 1995) or 48 (GEOS3 for 1998) sigma vertical layers. We retain this spatial resolution in the GEOS-CHEM simulation. The lowest model levels are centered at approximately 50, 250, 600, 1100, and 1750 m above the local surface in GEOS1 and 10, 50, 100, 200, 400, 600, 900, 1200, and 1700 m in GEOS3.

[7] The simulation of carbonaceous aerosols in GEOS-CHEM follows that of the Georgia Tech/Goddard Global Ozone Chemistry Aerosol Radiation and Transport (GOCART) model [*Chin et al.*, 2002], with a number of modifications described below. The model resolves EC and OC, with a hydrophobic and a hydrophilic fraction for each (i.e., four aerosol types). Combustion sources emit hydrophobic aerosols that then become hydrophilic with an e-folding time of 1.2 days following *Cooke et al.* [1999] and *Chin et al.* [2002]. We assume that 80% of EC and 50% of OC emitted from all primary sources are hydrophobic [*Cooke et al.*, 1999; *Chin et al.*, 2002; *Chung and Seinfeld*, 2002]. All secondary OC is assumed to be hydrophilic. The four aerosol types in the model are further resolved into contributions from fossil fuel, biofuel, and biomass burning, plus an OC component of biogenic origin, resulting in a total of 13 tracers transported by the model.

[8] Simulation of aerosol wet and dry deposition follows the schemes used by *Liu et al.* [2001] in previous GEOS-CHEM simulations of ^{210}Pb and ^{7}Be aerosol tracers. Wet deposition includes contributions from scavenging in convective updrafts, rainout from convective anvils, and rainout and washout from large-scale precipitation. Wet deposition is applied only to the hydrophilic component of the aerosol. Dry deposition of aerosols uses a resistance-in-series model [*Walcek et al.*, 1986] dependent on local surface type and meteorological conditions; it is small compared to wet deposition. *Liu et al.* [2001] found no systematic biases in their simulations of ^{210}Pb and ^{7}Be with GEOS-CHEM.

2.2. A Priori Sources of EC and OC

[9] We use global anthropogenic emissions of EC (6.4 Tg year^{-1}) and OC (10.5 Tg year^{-1}) from the gridded *Cooke et al.* [1999] inventory for 1984. This inventory includes contributions from domestic, vehicular, and industrial combustion of various fuel types. In the GOCART simulation of *Chin et al.* [2002], the *Cooke et al.* [1999] inventory was used with no seasonal variation. However, the source from heating fuel should vary with season [*Cabada et al.*, 2002]. *Cooke et al.* [1999] do not resolve the contributions to EC and OC emissions from heating fuel. We assume these contributions to represent 8% (EC) and 35% (OC) of total anthropogenic emissions, based on data for the Pittsburgh area from *Cabada et al.* [2002] and apply local seasonal variations of emissions using the heating degree days approach [*Energy Information Administration* (*EIA*), 1997; *Cabada et al.*, 2002]. In this manner we find that anthropogenic EC emission in the United States in winter is 15% higher than in summer. For OC the anthropogenic winter emission is twice that in summer.

[10] The *Cooke et al.* [1999] inventory does not include biofuels, which provide however an important source of heating in rural households and are also used in agro-industrial factories. We use a global biofuel use inventory with 1° × 1° spatial resolution from *Yevich and Logan* [2003] with emission factors of 1.0 g EC and 5 g OC per dry mass burned [*Streets et al.*, 2001; *Dickerson et al.*, 2002]. For the United States and Canada, we supersede that inventory with data on wood fuel consumption for residential and industrial sectors available for individual states and provinces [*EIA*, 2001] and which we distribute on a rural population map. Emission factors for this North American

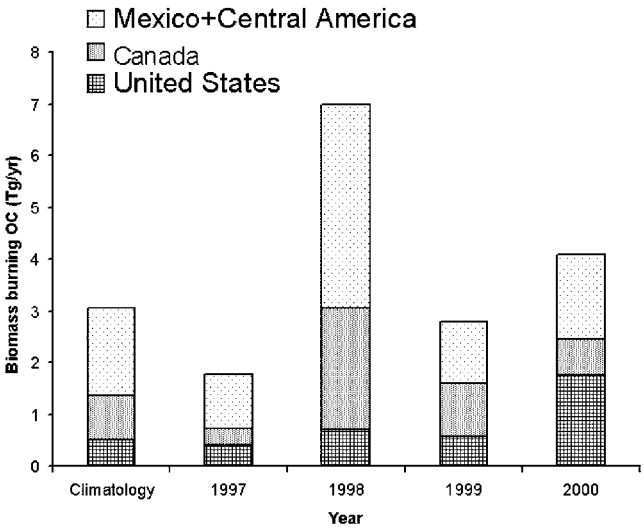

Figure 1. Yearly biomass burning OC emission in 1997–2000 for North and Central America, and climatological mean value (see section 2.2).

wood fuel source are 0.2 g EC and 3.0 g OC per kg dry wood burned [*Cabada et al.*, 2002]. Seasonal variation in biofuel emissions is included for the United States only and is estimated according to the heating degree-days approach.

[11] Biomass burning emissions of EC and OC are calculated using the global biomass burning inventory of *Duncan et al.* [2003]. This inventory uses a fire climatology compiled on a $1° \times 1°$ grid by *Lobert et al.* [1999], and applies monthly and interannual variability to that climatology from satellite observations. Emission factors are 2g EC and 14 g OC per kg dry mass burned [*Chin et al.*, 2002], higher than for biofuels because combustion is less efficient. For boreal forest fires, which are of particular interest here, emission factors reported in the literature range from 0.38 to 2.55 g EC per kg dry mass burned [*Lavoué et al.*, 2000, and references therein], consistent with the value assumed here. The OC/EC emission ratio of 7 is within the range of 6.9 to 8.2 used by *Liousse et al.* [1996]. Figure 1 shows the resulting annual OC emissions from biomass burning in North and Central America for 1997–2000 as well as the climatological mean. An ENSO-related drought resulted in catastrophic wildfires in the tropical forests of southern Mexico and Central America in 1998 [*Peppler et al.*, 2000]. Canadian fire emissions were also unusually large in 1998. Fire emissions in the United States were 38% higher than the climatological mean.

[12] Figure 2 shows the spatial and seasonal distribution of biomass burning OC emission from our model in 1998. Fires in Mexico and Central America were most intense in May [*Peppler et al.*, 2000, *Cheng and Lin*, 2001]. Canadian fires peaked in July–September. In the United States, most fires occurred in the northwest (Idaho, Montana) in summer; additional fires occurred in spring in Florida, owing to the ENSO-induced drought.

[13] Secondary formation of OC from oxidation of large hydrocarbons is an important source but uncertainties are large [*Griffin et al.*, 1999; *Kanakidou et al.*, 2000; *Chung and Seinfeld*, 2002]. *Chung and Seinfeld* [2002] find that biogenic terpenes are the main source of secondary OC aerosols. We assume a 10% carbon yield of OC from terpenes [*Chin et al.*, 2002], and apply this yield to a global terpene emission inventory dependent on vegetation type, monthly adjusted leaf area index, and temperature [*Guenther et al.*, 1995].

[14] Table 1 shows a summary of a priori EC and OC emissions used in the GEOS-CHEM simulation for 1998. The most important global source for both is biomass burning. In the United States, EC is mostly emitted from the combustion of fossil fuel and OC originates mostly from vegetation (but with large seasonal variation, as discussed below).

3. Model Evaluation

[15] A global evaluation of the EC and OC aerosol simulation was done by *Chin et al.* [2002] as part of a more general evaluation of aerosol optical depth using ground and satellite observations. Our simulation of aerosol sources and meteorological processes is similar to that of *Chin et al.* [2002] and our global distributions of EC and OC concentrations are comparable. We focus here our model evaluation on the United States, using observations at the IMPROVE sampling sites. The IMPROVE monitoring program was initiated in 1987 in national parks and other protected environments to identify the contribution of different aerosol components to visibility degradation [*Malm et al.*, 1994].

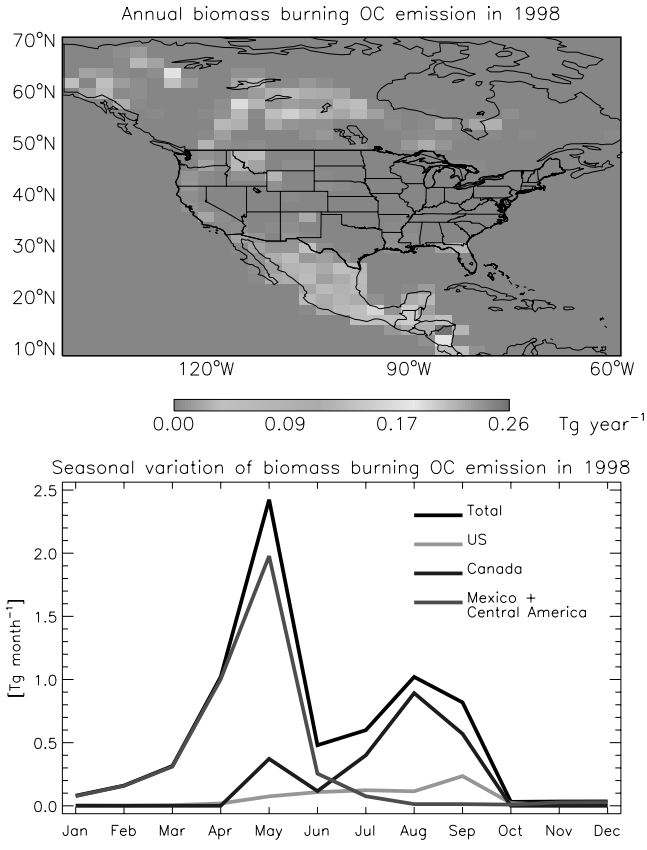

Figure 2. Annual biomass burning OC emission over North and Central America in 1998 (top) and seasonal variations for different regions (bottom). See color version of this figure at back of this issue.

Table 1. Carbonaceous Aerosol Sources in the GEOS-CHEM Model (1998)

Aerosol Source Type	Global,[a] Tg year^{-1}	United States, Tg year^{-1}	
		A Priori	A Posteriori
EC	22.0	0.66	0.75
Fossil fuel	6.6	0.52	0.60
Biofuel	1.4	0.04	0.07
Biomass burning	14.0	0.10	0.08
OC	129.8	2.70	3.11
Fossil fuel	10.6	0.45	0.52
Biofuel	7.6	0.54	0.89
Biomass burning	97.9	0.72	0.60
Biogenic	13.7	0.99	1.10

[a]Including a posteriori emissions for the United States.

The data for 1995 and 1998 consist of 24-hour speciated aerosol concentrations measured twice a week. The EC and OC concentrations are determined using the Thermal Optical Reflectance (TOR) method, which is state of the science but is subject to uncertainties that are difficult to quantify [*Chow et al.*, 1993; *Malm et al.*, 1994]. In the present paper we take the data at face value. There are 45 IMPROVE sites with continuous measurements for 1998 (Figure 3).

[16] Figure 4 compares simulated and observed annual mean EC and OC concentrations at the 45 IMPROVE sites for the year 1998. The IMPROVE measurements are plotted on the $2^\circ \times 2.5^\circ$ model grid. The bottom panels show the differences (model bias). A general objection to evaluating model results with 24-hour averaged concentrations in continental surface air is the inability of models to resolve nighttime stratification [*Jacob et al.*, 1993]. This is not an issue in our case because of high vertical resolution of the model near the surface and because the IMPROVE sites are not in the vicinity of large sources. We verified that the 24-hour average concentrations simulated by the model in layers 1 (0–10 m), 2 (10–50 m), and 3 (50–100 m) are not significantly different.

[17] Observed concentrations of EC and OC are generally higher in the eastern than the western United States, reflecting higher anthropogenic and vegetative (OC) emissions in the east. The OC maximum is shifted south relative to the EC maximum, and shows a secondary maximum along the west coast, reflecting the vegetative source. The model captures well this large-scale spatial distribution of EC and OC. Fires in the model also lead to high concentrations over Central America and western Canada.

[18] Site-to-site comparisons reveal however some major discrepancies between model and observations, as shown in the bottom panel of Figure 4 and in the scatterplot of Figure 5. Some of these discrepancies appear to reflect inadequate spatial resolution in the model. Model overestimates at coastal sites with large local urban or fire sources (BRIG in New Jersey; OKEF in Georgia; REDW, PORE, and PINN in California) are owing to the inability of the model to simulate steep subgrid land-to-sea gradients in mixing depth [*Fiore et al.*, 2002]. Model overestimates at SEQU (California) and GLAC (Montana) are due to local fire emissions (Figure 1) for which averaging over the grid scale may induce large errors in the simulation of local observations. We exclude these seven sites in further statistical data analysis.

[19] The model overestimates OC concentrations at THSI (Oregon) and MORA (Washington) sites owing to a particu-

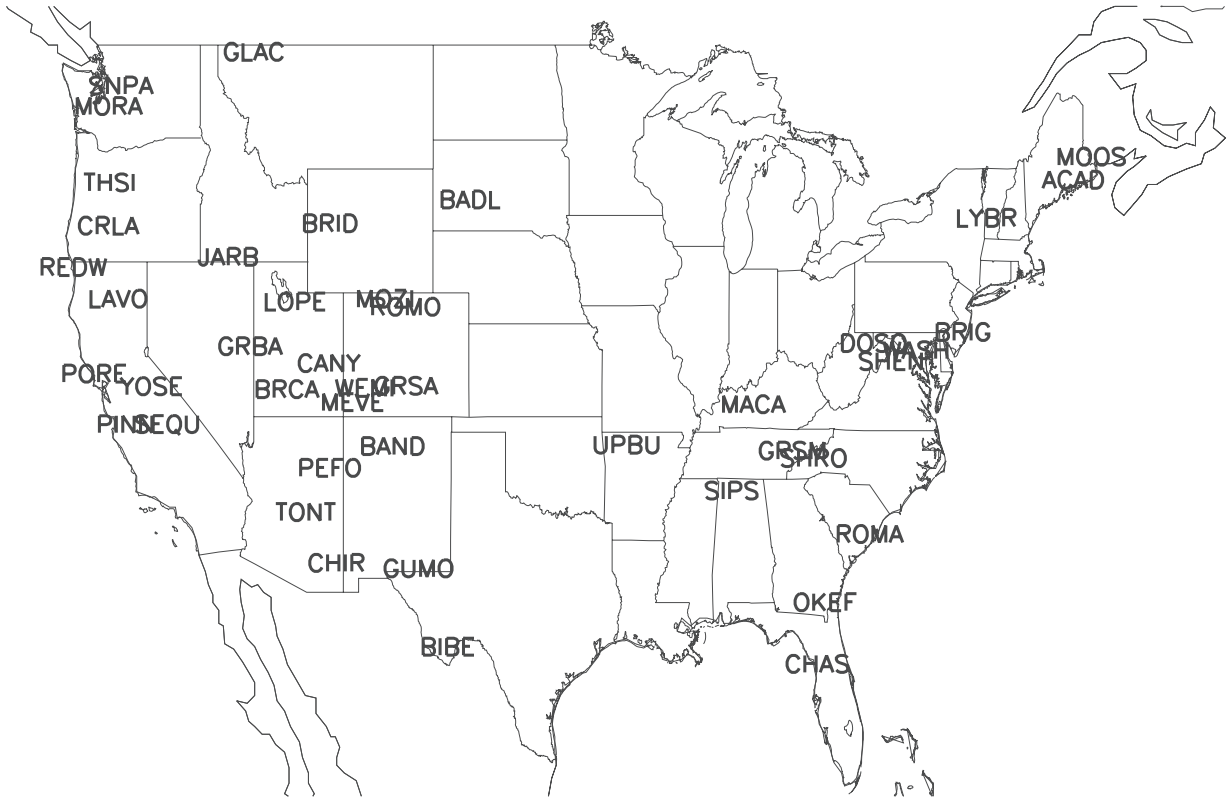

Figure 3. IMPROVE sampling sites with continuous records for 1998.

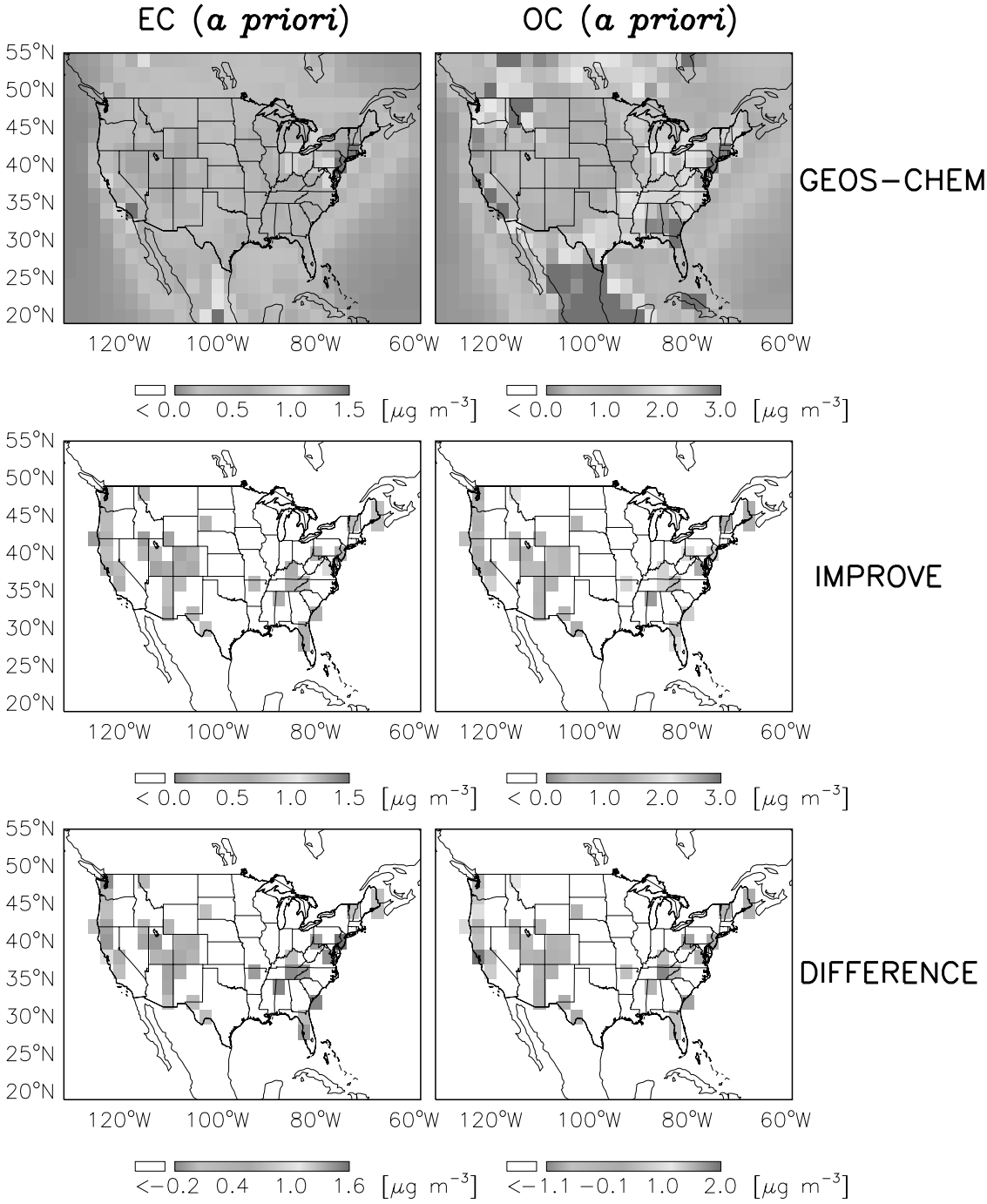

Figure 4. Annual mean concentrations of EC (left) and OC (right) in surface air over the United States in 1998. The top panels show results from the GEOS-CHEM model using a priori sources. The middle panels shows the IMPROVE observations plotted on the model 2° × 2.5° grid. The bottom panel shows the difference between the two. See color version of this figure at back of this issue.

larly large vegetative source in the model in summer that is apparently not seen in the observations. The discrepancy is local in nature (it is not found at nearby sites). As discussed further below, our specification of the vegetative OC source appears inadequate to describe OC concentrations at these two sites, and therefore we exclude them from further statistical analysis.

[20] Figure 5 shows that the model generally reproduces the annual mean EC and OC concentrations to within a factor of two and captures the spatial pattern well (R^2 = 0.84 for EC and R^2 = 0.67 for OC). However, the slope of the reduced major axis line [*Hirsch and Gilroy*, 1984] is 0.85 ± 0.06 for EC and 0.74 ± 0.08 for OC, reflecting a low bias in the model. We will correct for this model bias by adjusting the sources, as discussed below.

[21] Figures 6 and 7 compare seasonal variations of simulated and observed EC and OC concentrations at selected IMPROVE sites. Contributions from individual sources to the model concentrations are shown. Seasonal variations for EC differ considerably from site to site, and

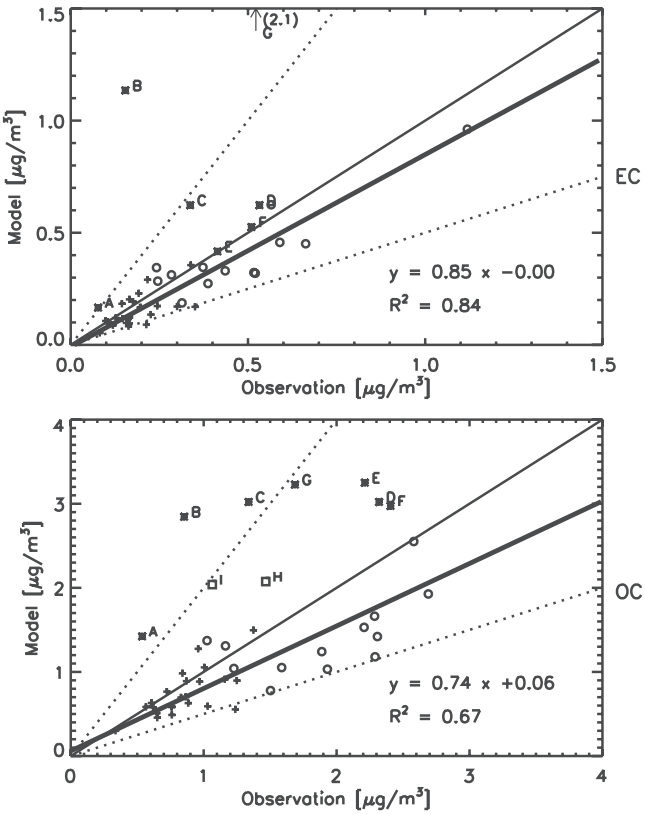

Figure 5. Scatterplot of simulated (GEOS-CHEM) versus observed (IMPROVE) annual mean EC and OC concentrations for the data shown in Figure 4. The pluses and the circles indicate data in the western and eastern United States (separated at 95°W), respectively. The asterisks with letter labels indicate sites discarded in the statistical analysis (see section 3): REDW(A), PORE(B), PINN(C), SEQU(D), GLAC(E), OKEF(F), and BRIG(G). The squares indicate OC data at MORA(H) and THSI(I) sites which were discarded in statistical analysis for OC. The thin solid and dotted lines represent the y = x relation and a factor of 2 deviation. The thick solid line represents the reduced major axis linear regression [*Hirsch and Gilroy*, 1984], excluding sites A-I. The Pearson correlation coefficients R^2 and regression equations are indicated.

the model has significant success in capturing these differences. Fossil fuel is the dominant source for EC at most sites, but seasonal maxima in May–September over the western United States are due to forest fires. The OC concentrations are generally highest in summer and lowest in winter, both in the model and in the observations; this seasonal variation is mostly due to the biogenic source. Peaks in OC in May–September in the western United States are seen both in the model and in the observations and are due to wildfires, as for EC. Wintertime OC is higher in the eastern than the western United States, and includes contributions of comparable importance from biofuels and fossil fuels.

[22] *Rogers and Bowman* [2001] used satellite measurements and air parcel trajectory calculations to illustrate the transport of the 1998 fire plumes from Central America to the central and southern United States. Our model successfully captures the corresponding peaks of EC and OC observed in May at the IMPROVE sites (e.g., BIBE in Texas, CHIR in Arizona, CANY in Utah, MOZI in Colorado, UPBU in Arkansas, GRSM in Tennessee). The enhancement in concentrations is much stronger for OC than for EC, both in the model and in the observations, reflecting high OC/EC fire emission ratios and the relatively large fossil fuel source of EC in the United States.

[23] The model has also some success in reproducing the influences from fire emissions within the United States. For example, the high OC in April–June at CHAS in Florida is well captured in the model. Fires in the western United States result in peak EC and OC concentrations in September at several sites (MORA, Washington; THSI, Oregon; LAVO, California; JARB, Nevada).

[24] Figure 8 compares simulated and observed monthly mean concentrations for the ensemble of IMPROVE sites and for separate seasons. The model simulation with a priori sources has success in reproducing the variability of observed EC and OC for winter and spring, as measured by the high R^2 (0.67–0.79) correlation between model and observations. The slope of the regression line (0.84–0.98) is close to one for both EC and OC. The R^2 is lower in summer and fall, particularly for OC (0.37–0.40) and the slope of the regression line is off from one (0.72–0.74 for EC and 0.74–1.06 for OC). The slope of the OC regression line in fall is close to one only because high model bias from wildfire sources at western sites offsets the low model bias at eastern sites.

4. Top-Down Emission Estimates

[25] The statistical model biases apparent in Figure 8 could reflect errors in the a priori sources. We examine what adjustments in the sources would be needed for least squares minimization of the bias between simulated and observed monthly mean EC and OC concentrations. We identify for this purpose four source components: fossil fuel, biofuel, biomass burning, and vegetation (the latter for OC only). We use a multiple linear regression to fit the annual mean U.S. source for each component to the monthly mean IMPROVE observations. In order to give equal weight to EC and OC concentrations in the least squares minimization, we normalize them by their respective annual mean concentrations for the ensemble of IMPROVE sites (0.29 μg m^{-3} for EC, 1.23 μg m^{-3} for OC).

[26] We find in this manner that fossil fuel and biofuel emissions should be increased by 15% and 65% respectively from a priori levels, while biomass burning emissions should be decreased by 17% and the biogenic source for OC should be increased by 11%. We consider these adjustments to be well within the uncertainties on the a priori estimates. The a posteriori values of our adjusted sources are given in Table 1. The increase in the biofuel source is largely determined by the model underestimate of observed OC for the cold season.

[27] Figure 9 presents annual mean surface air concentrations of EC and OC in the model using a posteriori sources. Relative to the simulation with a priori sources (Figure 4), there are 15–20% increases in EC and OC concentrations in the eastern United States. Changes in the western United States are smaller because the decrease in

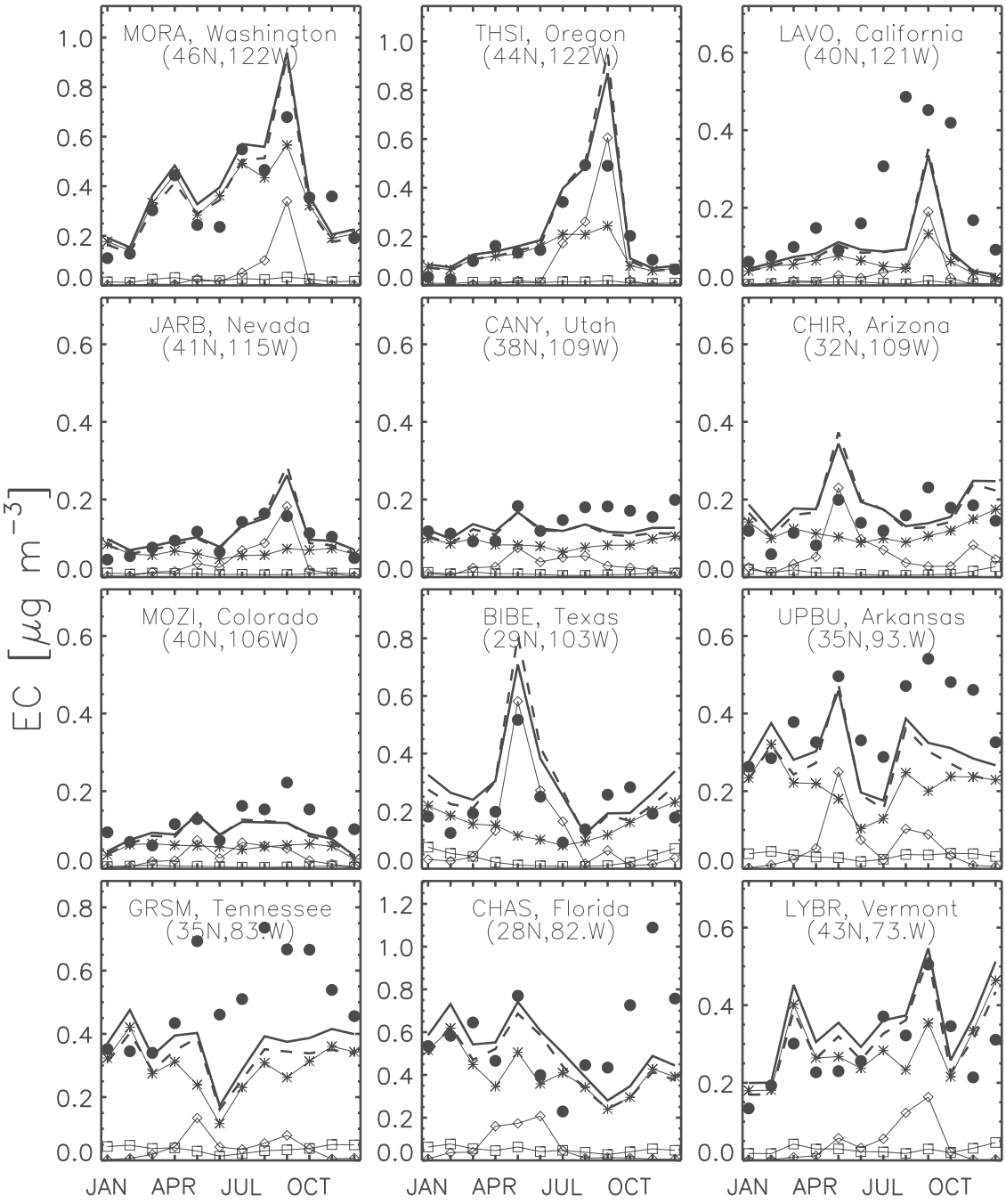

Figure 6. Seasonal variation of monthly mean EC concentrations in 1998 at selected IMPROVE sites. Site locations are shown in Figure 1. Values are monthly means. Closed circles indicate the observations. Dashed and solid lines represent the model simulations with a priori and a posteriori sources, respectively. The a priori model components by source types are indicated as thin solid lines with symbols: asterisks (fossil fuel combustion), diamonds (biomass burning), and squares (biofuel use).

the biomass burning source offsets the increase in the biogenic OC source.

[28] The effect of source adjustment on the ability of the model to fit observed EC and OC concentrations is shown by the scatterplots in Figure 8. Compared to the simulation with a priori sources, the R^2 correlation coefficients are slightly higher and the slopes of the regression lines are closer to unity. Figures 6 and 7 show the effect of the a posteriori sources on the simulation at individual sites. The adjustments are generally too small to correct site-specific discrepancies, which would require modifying the geographic distributions of the sources.

[29] Figures 10 and 11 show the contributions of individual a posteriori sources to EC and OC for winter and summer. Fossil fuel is the most important source of EC everywhere in the United States, except in some areas in the west in summer where wildfires make a more important contribution. For OC, the anthropogenic sources (fossil and biofuel) dominate in winter, while the natural sources (fires and vegetation) are more important in summer. The fossil

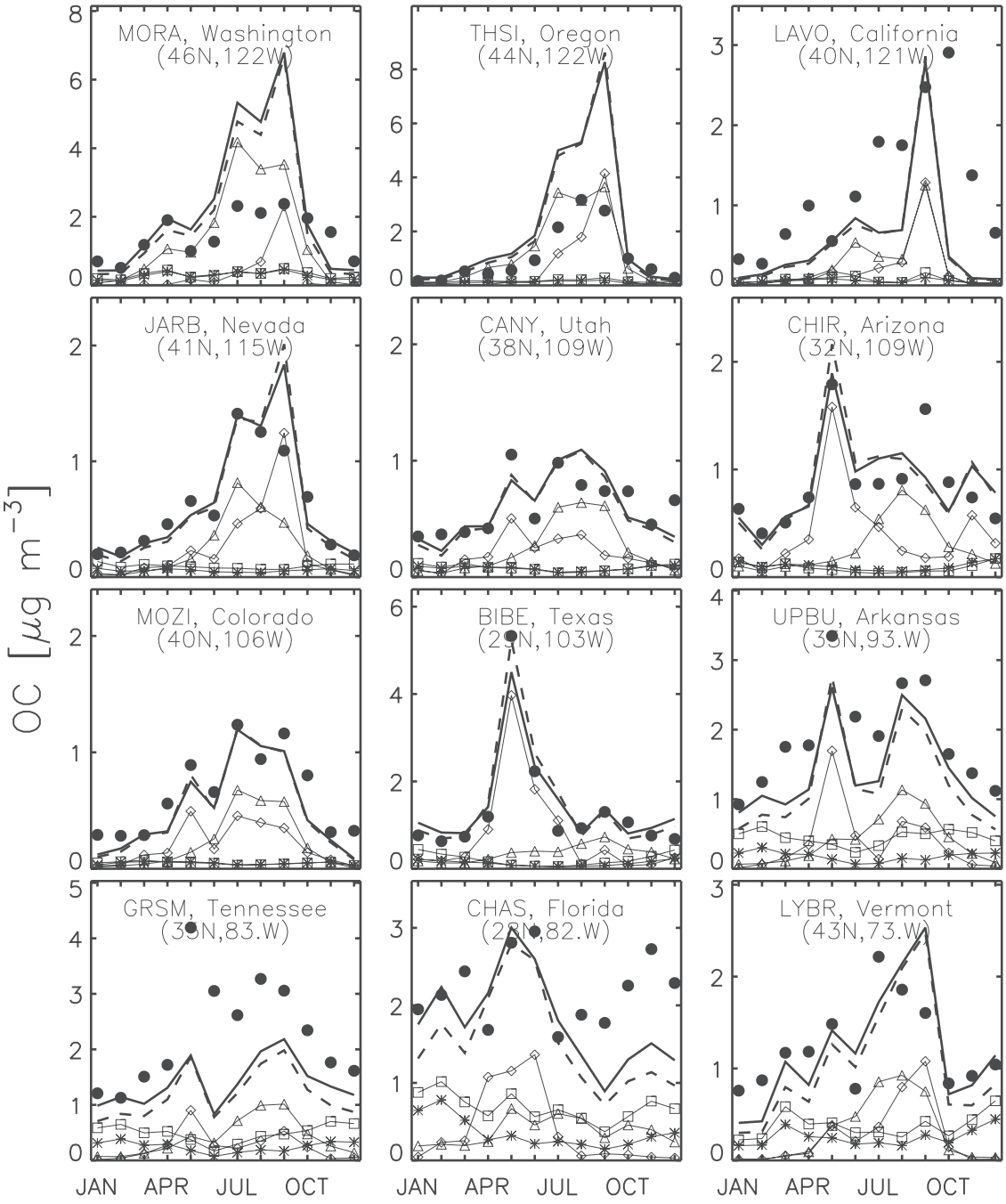

Figure 7. Same as in Figure 6 but for OC. The a priori model results by source types are represented as thin solid line with asterisks (fossil fuel), diamonds (biomass burning), squares (biofuel), and triangles (biogenic terpenes).

fuel OC is mostly concentrated in the northeastern corridor, the industrial midwest and southern California, whereas the biofuel OC is more widely distributed. Biogenic OC in summer is highest in the southeast and along the west coast. We previously discussed in the context of Figure 7 the large OC enhancements in the southern United States due to fires in Central America, but these enhancements are in spring (cf. Figure 2) and thus not apparent in Figure 11. Figure 11 shows a large enhancement in OC concentrations over the north-central United States due to Canadian fires, but the IMPROVE sites are not well situated to observe this enhancement (Figure 3). We present below a case study for summer 1995 demonstrating Canadian fire influence over the eastern United States.

5. Canadian Fire Influence: A Case Study for the Summer of 1995

[30] Previous studies [*Wotawa and Trainer*, 2000; *Fiore et al.*, 2002; *McKeen et al.*, 2002] have shown that major Canadian wildfires in June–July 1995 caused large enhancements of CO and smaller enhancements of ozone

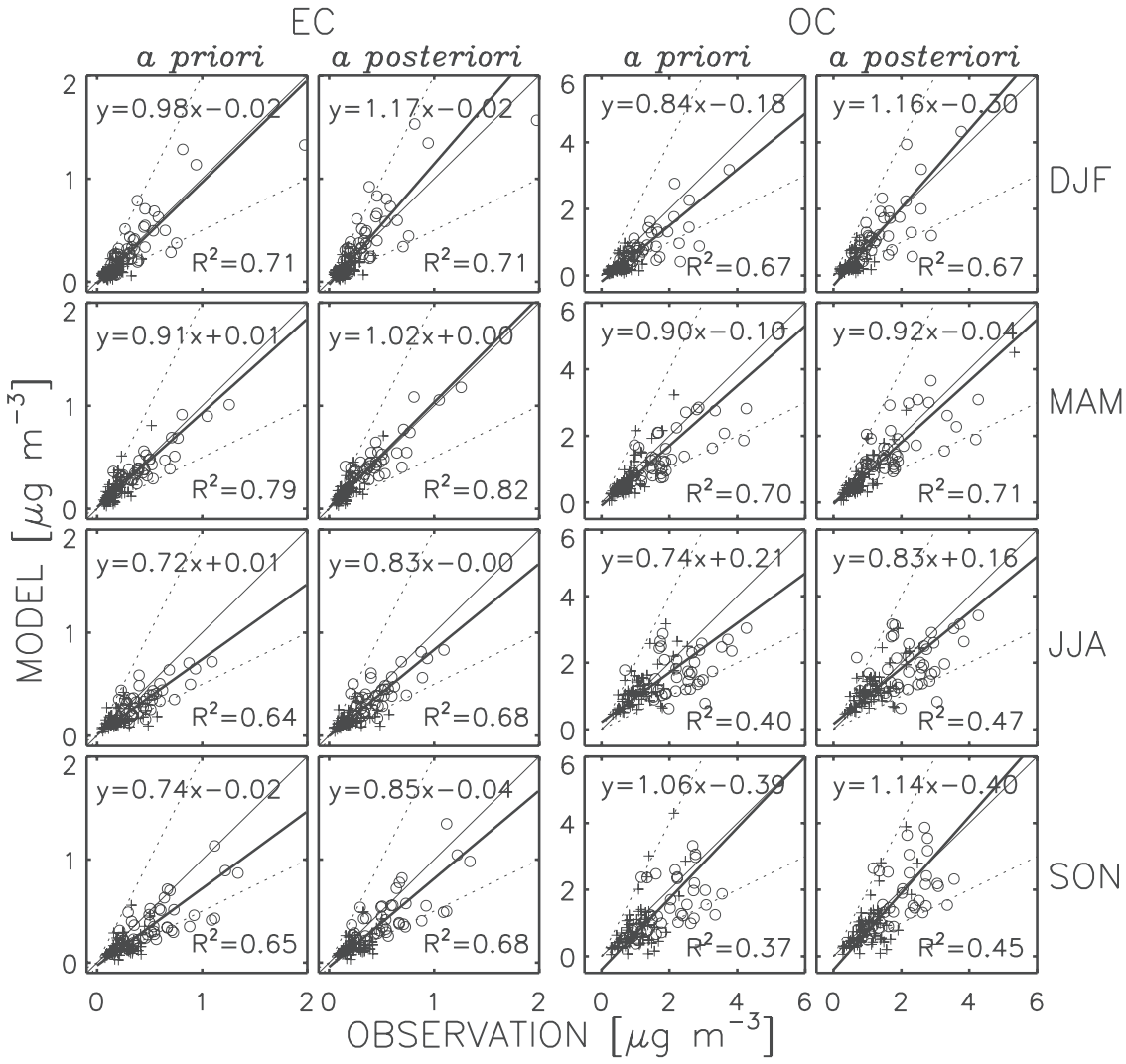

Figure 8. Scatterplots of monthly mean EC (left two columns) and OC (right two columns) simulated versus observed concentrations with a priori (left) and a posteriori (right) sources, for the ensemble of IMPROVE sites and for individual seasons in 1998. Sites in the western and eastern United States (separated at 95°W) are shown as pluses and open circles, respectively. Thin solid lines indicate a perfect match of the model results with observations, and dotted lines denote a factor of 2 departure. Thick solid lines represent the reduced major axis regression. The Pearson correlation coefficients R^2 are indicated.

in the southeastern United States. The Canadian fire plumes were carried by northerly flows associated with high-pressure systems on the back side of cold fronts. We use here a GEOS-CHEM simulation for the summer 1995 to demonstrate large aerosol EC and OC enhancements from these fires at IMPROVE sites in Arkansas (UPBU), Tennessee (GRSM) and Kentucky (MACA).

[31] Our simulation of the 1995 Canadian wildfires uses daily, geographically resolved emission data estimated from the area burned in each province. Those data are given by *Wotawa and Trainer* [2000] for CO, and are scaled here to our climatological biomass burning emission inventory for CO [*Lobert et al.*, 1999] to derive corresponding EC and OC emissions. The resulting EC and OC emissions from the fires are 0.34 and 2.41 Tg, respectively, and are distributed in five areas (Northwest Territories, Alberta, Saskatchewan, Manitoba, and Ontario) for four burning periods from 17 June to 13 July.

[32] Figure 12 shows the time series of simulated and observed EC and OC concentrations at three sites in the southeastern United States: UPBU in Arkansas, MACA in Kentucky, and GRSM in Tennessee. There are two large peaks in the observations, for 1 and 8 July, which are captured by the model and are due to the Canadian fires (compare solid and dashed lines in Figure 12). The timing of those peaks is consistent with those concurrently observed for CO at nearby sites [*McKeen et al.*, 2002]. Our simulation of the magnitude of the 7–9 July event is improved in a sensitivity simulation where we assume initial lifting of the fire emissions up to 4 km altitude (Figure 12, dotted line). Such lifting can be expected from buoyancy, particularly for large crown fires [*Liousse et al.*, 1996, 1997; *Lavoué et al.*, 2000].

[33] Our model simulation allows us to assess the influence of Canadian fire emissions on seasonal aerosol concentrations in the United States for the summer of 1995. We

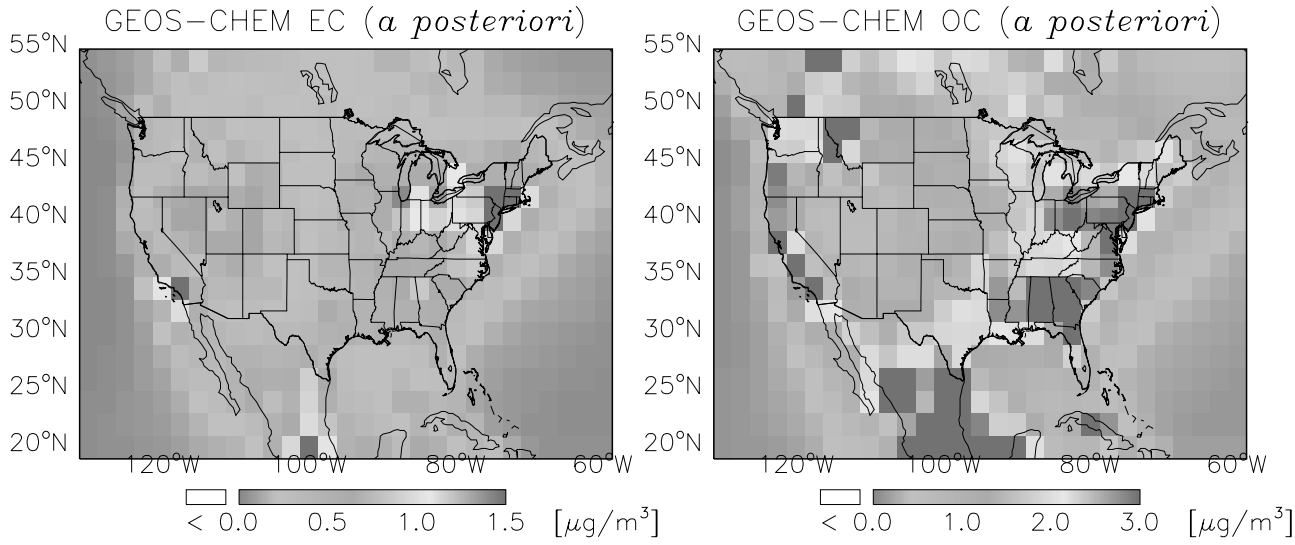

Figure 9. Annual mean concentrations of EC (left) and OC (right) in surface air over the United States in 1998 from the GEOS-CHEM model using a posteriori sources. See color version of this figure at back of this issue.

find that the events associated with Canadian fire plumes persisted typically for 3–5 days. On a seasonal basis, they caused the mean June–August 1995 natural EC to increase by 80% (east) and 36% (west) and the mean OC to increase by 23% (east) and 16% (west), relative to a sensitivity simulation with no Canadian fires.

6. Implications for Natural Visibility in the United States

[34] We use results from our model to estimate the role of natural carbonaceous aerosols in visibility reduction and compare to the default values recommended by *EPA* [2001] for application of the regional haze rule. Our 1998 simulation with a posteriori sources yields annual average concentrations of natural EC and OC from fires and vegetation of 0.09 $\mu g/m^3$ and 1.09 $\mu g/m^3$, respectively, for the western United States (west of 95°W) and 0.06 $\mu g/m^3$ and 0.95 $\mu g/m^3$, respectively, for the eastern United States. In order to compute the light extinction by OC we need to multiply the OC mass by 1.4 to obtain an Organic Carbon Mass (OMC) that accounts for the noncarbon additional mass attached to OC aerosols [*Malm et al.*, 1994]. The resulting annual average for natural OMC is 1.52 $\mu g/m^3$ and 1.33 $\mu g/m^3$ for the west and east, respectively. Except for OMC in the eastern United States, our best estimates of natural concentrations for EC and OMC are significantly higher than the default values recommended by *EPA* [2001] which are 0.02 $\mu g/m^3$ for EC, and 0.47 $\mu g/m^3$ (west) and 1.40 $\mu g/m^3$ (east) for OMC.

[35] Several issues need to be addressed in this comparison to the EPA default values. First, 1998 had unusually high fire emissions, principally from Mexico and Canada, as shown in Figure 1. Second, it is important to quantify the contribution of transboundary transport to natural EC and OC concentrations in the United States. Third, there is ambiguity from a U.S. policy standpoint as to whether intercontinental transport of anthropogenic pollution (as from Asia) should be considered part of the "natural" background. To address these issues we conducted three sensitivity simulations, with sources modified from those in our standard 1998 simulation. The first includes no EC and OC sources in the United States to quantify the contributions from transboundary transport, mostly from Canada and Mexico. The second includes EC and OC sources from Asia only, to quantify the transpacific transport. The third uses climatological biomass burning emissions as shown in Figure 1 in order to derive mean default values of natural EC and OC concentrations in the United States. The results are summarized in Table 2.

[36] We find that the transboundary transport of anthropogenic sources makes only a small contribution (less than 10%) to the total anthropogenic concentrations of EC and OC in the United States. However, the transboundary transport of natural sources, mostly from fires in Canada and Mexico, makes a large contribution to annual mean natural concentrations in the United States for 1998 (44% in the west and 67% in the east for EC; 28% in the west and 37% in the east for OC).

[37] Transpacific transport from Asian sources is found to make little contribution to EC and OC concentrations in the United States, even in the context of the natural background. The concentrations generated in the simulation with anthropogenic and natural Asian sources only (Table 2) amount to less than 2% of the natural OC concentrations from the standard simulation, and less than 10% of the natural EC. The small role of intercontinental transport in contributing to background EC and OC concentrations over the United States reflects the short lifetime of these species against wet deposition, particularly considering that the lifting of air from the continental boundary layer to the free troposphere involves wet processes [*Stohl*, 2001]. This can be contrasted to ozone, for which transport from outside North America makes a large contribution to the U.S. background [*Fiore et al.*, 2002].

[38] Our best estimates of mean natural EC and OC concentrations for comparison to the EPA default values are obtained from the simulation using mean climatological

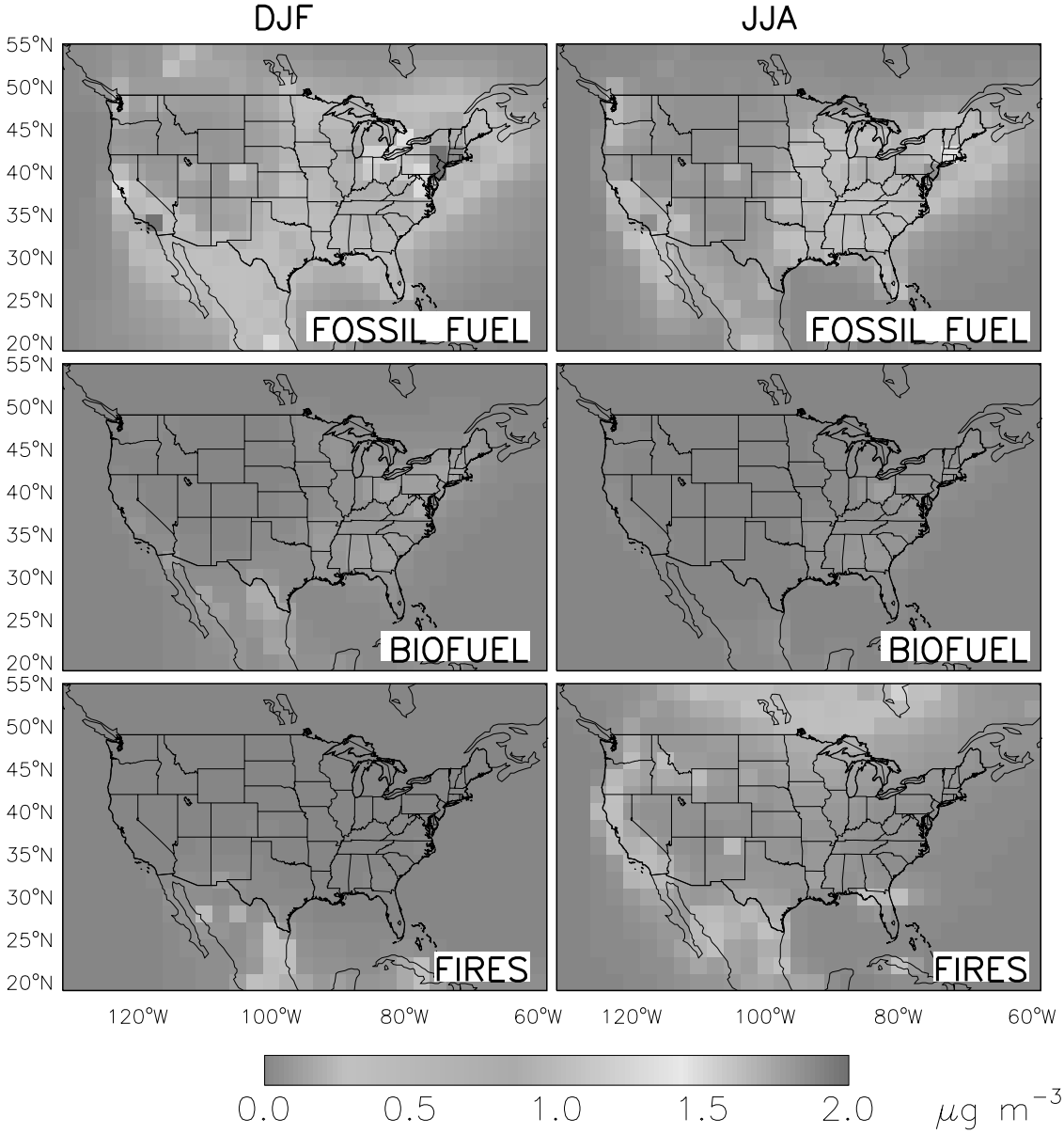

Figure 10. Contribution from different sources types to EC concentrations ($\mu g\ m^{-3}$) in surface air for DJF and JJA. Values are model results for 1998 using a posteriori sources (Table 1). See color version of this figure at back of this issue.

fire emissions. We find annual average concentrations of natural EC and OMC of 0.06 $\mu g/m^3$ and 1.25 $\mu g/m^3$, respectively, for the western United States and 0.04 $\mu g/m^3$ and 1.17 $\mu g/m^3$, respectively, for the eastern United States (Table 2). These are higher by a factor of 2–3 than the EPA default values except for OMC in the eastern United States which is lower by 16%.

[39] The implications of our results for natural visibility estimates are substantial, particularly in the western United States. Our higher natural OMC component relative to EPA's default estimates results in lower natural visibility. For example, *EPA* [2001] uses its default natural PM concentrations to derive mean light extinctions of $15.60 \times 10^{-6}\ m^{-1}$ and $15.78 \times 10^{-6}\ m^{-1}$ at Bandelier National Monument (BAND, New Mexico) and at Yellowstone National Park (YELL, Wyoming). Applying the *EPA* [2001] visibility formula with our best estimates of natural EC and OMC (from the simulation with climatological mean fires), and using EPA default values for the other PM components, we find natural light extinctions of $19.13 \times 10^{-6}\ m^{-1}$ and $19.31 \times 10^{-6}\ m^{-1}$ at BAND and YELL, respectively, about 22% higher than EPA values.

7. Conclusions

[40] We used the GEOS-CHEM global 3-D model to simulate observed concentrations of elemental carbon (EC) and organic carbon (OC) from a network of 45 sites in relatively remote regions of the United States (IMPROVE network). Our focus was to better quantify the anthropogenic and natural sources of EC and OC in the United States, and the role of transboundary and intercontinental

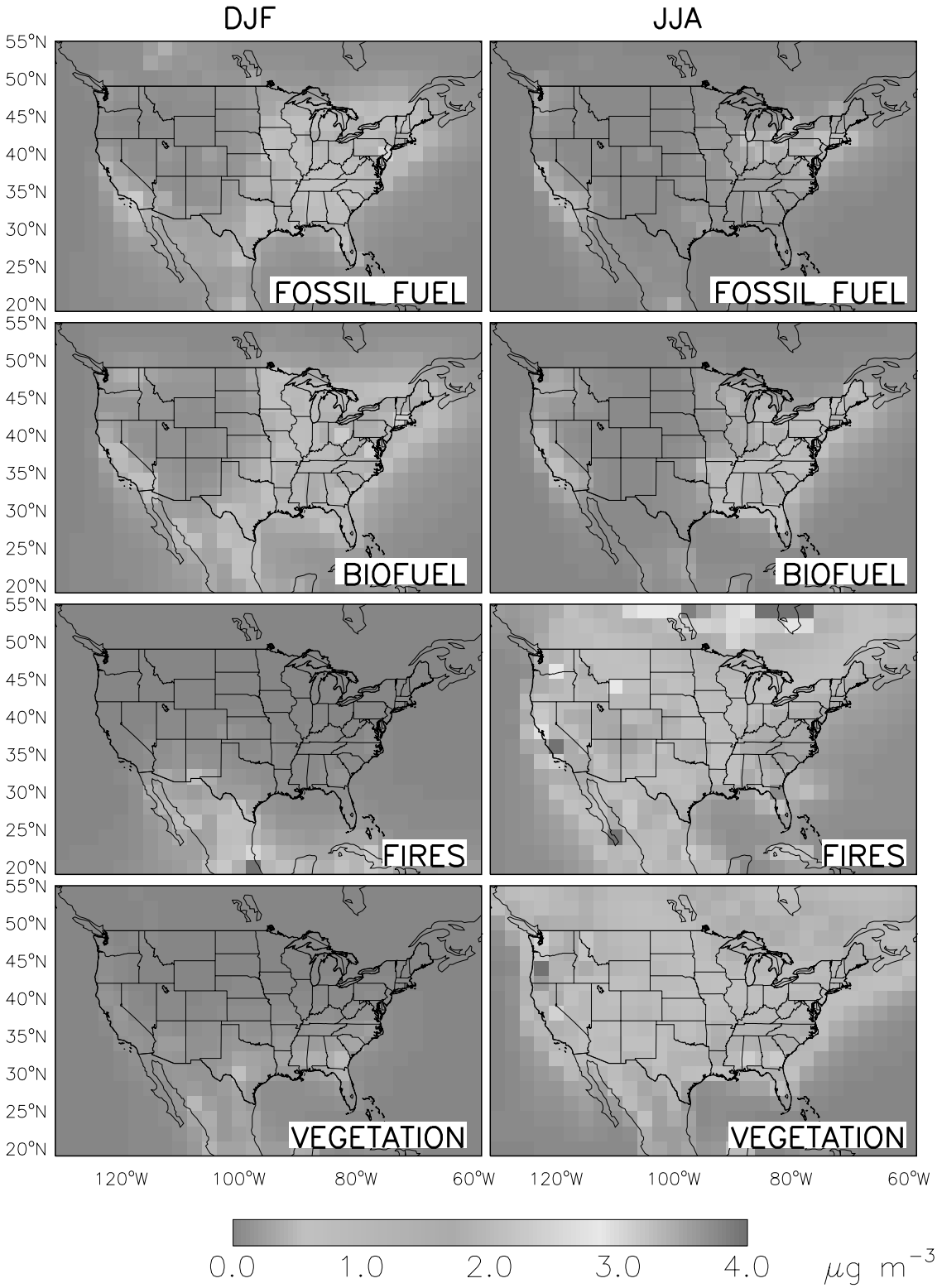

Figure 11. Same as Figure 10 but for OC. See color version of this figure at back of this issue.

transport, in the context of assessing the effect of these aerosols on visibility.

[41] We conducted a 1-year simulation for 1998 using best a priori estimates of EC and OC sources, including global satellite observations of fires, and compared the results to observed concentrations at the IMPROVE sites. Wildfire emissions were from a gridded climatological inventory, scaled to monthly fire emissions for 1998 using satellite fire count data. The model reproduces well the spatial pattern in the observations ($R^2 = 0.84$ for EC, $R^2 = 0.67$ for OC) but is biased low by 15% for EC and 26% for OC. From a multiple linear regression fit we concluded that fossil fuel and biofuel emissions for EC and OC in the United States should be increased by 15%, and 65%

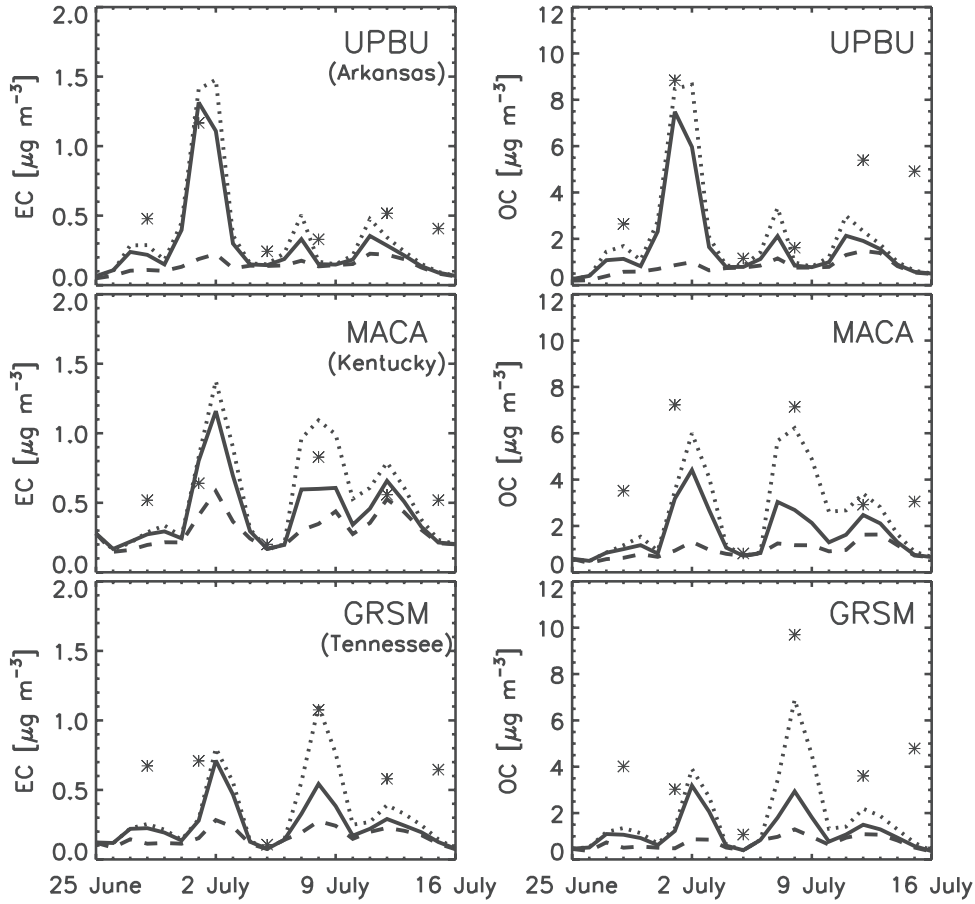

Figure 12. Concentrations of EC and OC at three southeastern U.S. sites (UPBU, MACA, and GRSM) in June–July 1995. Observations (24-hour averages, twice a week) are shown as asterisks. The solid line shows results from the standard model simulation. Results from sensitivity simulations without Canadian fire emissions (dashed line) and with fire emissions initially mixed to 600 hPa (dotted line) are also shown.

respectively from a priori levels, while biomass burning emissions for both EC and OC should be decreased by 17% and the biogenic source for OC should be increased by 11%. Our best a posteriori estimates are given in Table 1.

[42] Canadian fire influence on the United States in 1998 was largely confined to the upper midwest, where no IMPROVE data are available. We conducted an additional simulation for the summer of 1995, for which large CO enhancements in the southeastern United States from Canadian fires had previously been reported [*Wotawa and Trainer*, 2000]. We find correspondingly large EC and OC enhancements in the IMPROVE observations for this region, which the model captures and diagnoses as being due to Canadian fire emissions. Model results indicate that Canadian fires in 1995 enhanced the mean June–August natural EC and OC concentrations in the eastern United States by 80% and 23%, respectively.

[43] Our 1998 and 1995 simulations lead confidence in the representation of fire emissions of EC and OC in the model. We used a simulation with climatological monthly mean fire emissions, together with our best estimate of the biogenic OC source, to estimate natural concentrations of carbonaceous aerosols in the United States for purpose of natural visibility assessments and application of the EPA regional haze rule [*EPA*, 2001]. Our best estimates of natural

Table 2. Natural and Anthropogenic EC and OC Concentrations ($\mu g\ m^{-3}$) in the United States[a]

	Natural Concentrations		Anthropogenic Concentrations	
	West	East	West	East
EC				
1998 emissions (base)	0.09	0.06	0.21	0.62
No U.S. sources	0.04	0.04	0.02	0.02
Asian sources only	0.003	0.001	0.005	0.003
Climatological fire emissions	0.06	0.04	0.21	0.62
OMC[b]				
1998 emissions (base)	1.52	1.33	0.52	1.90
No U.S. sources	0.43	0.49	0.05	0.05
Asian sources only	0.022	0.013	0.013	0.007
Climatological fire emissions	1.25	1.17	0.52	1.90

[a]Values are annual means from the standard 1998 simulation (base) and from the sensitivity simulations described in section 5. Partition between west and east is at 95°W. The natural concentrations from the simulation with climatological fire emissions can be compared to the default estimates suggested by *EPA* [2001] for application of the regional haze rule: 0.47 $\mu g\ m^{-3}$ (west) and 1.40 $\mu g\ m^{-3}$ (east) for OMC, and 0.02 $\mu g\ m^{-3}$ for EC.

[b]Organic carbon mass (OMC), defined as 1.4 times the OC mass to account for noncarbon contributions to the organic aerosol.

annual mean concentrations for EC are 0.06 $\mu g/m^3$ in the western United States (west of 95°W) and 0.04 $\mu g/m^3$ in the east; for organic carbon mass (OMC = 1.4 OC, to account for the noncarbon contribution to OC aerosols), they are 1.25 $\mu g/m^3$ in the west and 1.17 $\mu g/m^3$ in the east. These values are 2–3 times higher than the default values recommended by *EPA* [2001] for application of the regional haze rule, except for OMC in the east (16% lower). Our higher estimates of the natural OMC concentrations relative to EPA's default estimates result in higher natural light extinction (and hence lower natural visibility) by 22% in the western United States. We also find a large seasonal variability in natural light extinction from EC and OC, with highest values in summer owing to sources from wildfires and vegetation.

[44] We further investigated the contribution from transboundary transport to EC and OC concentrations in the United States. A sensitivity simulation with no EC and OC sources in the United States shows that fires in Mexico and Canada made a large contribution to annual mean natural concentrations of EC (40–70%) and OC (30–40%) in the United States in 1998. A sensitivity simulation with Asian sources only shows that transpacific transport contributes less than 10% of the natural background EC over the United States, and less than 2% of the natural background OC.

[45] **Acknowledgments.** This research was supported by the Electric Power Research Institute (EPRI) and the U.S. Environmental Protection Agency (EPA). The authors are grateful to R. Yevich for providing her annual biofuel emission data.

References

Bey, I., D. J. Jacob, R. M. Yantosca, J. A. Logan, B. Field, A. M. Fiore, Q. Li, H. Liu, L. J. Mickley, and M. Schultz, Global modeling of tropospheric chemistry with assimilated meteorology: Model description and evaluation, *J. Geophys. Res.*, *106*, 23,073–23,096, 2001.

Cabada, J. C., S. N. Pandis, and A. L. Robinson, Sources of atmospheric carbonaceous particulate matter in Pittsburgh, Pennsylvania, *J. Air Waste Manage. Assoc.*, *52*, 732–741, 2002.

Cheng, M.-D., and C.-J. Lin, Receptor modeling for smoke of 1998 biomass burning in Central America, *J. Geophys. Res.*, *106*, 22,871–22,886, 2001.

Chin, M., P. Ginoux, S. Kinne, O. Torres, B. Holben, B. N. Duncan, R. V. Martin, J. A. Logan, A. Higurashi, and T. Nakajima, Tropospheric aerosol optical thickness from the GOCART model and comparisons with satellite and sunphotometer measurements, *J. Atmos. Sci.*, *59*, 461–483, 2002.

Chow, J. C., J. G. Watson, L. C. Pritchett, W. R. Pierson, C. A. Frazier, and R. G. Purcell, The DRI thermal/optical reflectance carbon analysis system: Description, evaluation and applications in U.S. air quality studies, *Atmos. Environ., Part A*, *27*, 1185–1201, 1993.

Chung, S. H., and J. H. Seinfeld, Global distribution and climate forcing of carbonaceous aerosols, *J. Geophys. Res.*, *107*(D19), 4407, doi:10.1029/2001JD001397, 2002.

Cooke, W. F., C. Liousse, H. Cachier, and J. Feichter, Construction of a 1° × 1° fossil fuel emission data set for carbonaceous aerosol and implementation and radiative impact in the ECHAM-4 model, *J. Geophys. Res.*, *104*, 22,137–22,162, 1999.

Dickerson, R. R., M. O. Andreae, T. Campos, O. L. Mayol-Bracero, C. Neusuess, and D. G. Streets, Analysis of black carbon and carbon monoxide observed over the Indian Ocean: Implications for emissions and photochemistry, *J. Geophys. Res.*, *107*(D19), 8017, doi:10.1029/2001JD000501, 2002.

Duncan, B. N., R. V. Martin, A. C. Staudt, R. Yevich, and J. A. Logan, Interannual and seasonal variability of biomass burning emissions constrained by satellite observations, *J. Geophys. Res.*, *108*(D2), 4100, doi:10.1029/2002JD002378, 2003.

Energy Information Administration (EIA), *State Energy Data Report 1999*, Washington, D. C., 2001.

Environmental Protection Agency (EPA), Draft guidance for estimating natural visibility conditions under the regional haze rule, *U.S. EPA OAQPS Report*, Washington, D. C., 27 Sept. 2001.

Fiore, A. M., D. J. Jacob, I. Bey, R. M. Yantosca, B. D. Field, A. C. Fusco, and J. G. Wilkinson, Background ozone over the United States in summer: Origin, trend, and contribution to pollution episodes, *J. Geophys. Res.*, *107*(D15), 4275, 10.1029/2001JD000982, 2002.

Griffin, R. J., D. Dabdub III, and J. H. Seinfeld, Estimate of global atmospheric organic aerosol from oxidation of biogenic hydrocarbons, *Geophys. Res. Lett.*, *26*, 2721–2724, 1999.

Guenther, A., et al., A global model of natural volatile organic compound emission, *J. Geophys. Res.*, *100*, 8873–8892, 1995.

Hirsch, R. M., and E. J. Gilroy, Methods of fitting a straight line to data: Examples in water resourses, *Water Res. Bull.*, *20*, 705–711, 1984.

Jacob, D. J., et al., Simulation of summertime ozone over North America, *J. Geophys. Res.*, *98*, 14,797–14,816, 1993.

Kanakidou, M., K. Tsigaridis, F. J. Dentener, and P. J. Crutzen, Human-activity-enhanced formation of organic aerosols by biogenic hydrocarbon oxidation, *J. Geophys. Res.*, *105*, 9243–9254, 2000.

Lavoué, D., C. Liousse, and H. Cachier, Modeling of carbonaceous particles emitted by boreal and temperate wildfires at northern latitudes, *J. Geophys. Res.*, *105*, 26,871–26,890, 2000.

Liousse, C., J. E. Penner, C. Chuang, J. J. Walton, H. Eddleman, and H. Cachier, A global three-dimensional model study of carbonaceous aerosols, *J. Geophys. Res.*, *101*, 19,411–19,432, 1996.

Liousse, C., H. Cachier, and W. Guelle, Determining a global climatology for tropical biomass burning aerosols, paper presented at the 6th International Conference on Carbonaceous Particles, Austrian Fed. Minist. of Environ. and Sci. and Technol., Vienna, Sept. 1997.

Liu, H., D. J. Jacob, I. Bey, and R. M. Yantosca, Constraints from ^{210}Pb and ^{7}Be on wet deposition and transport in a global three-dimensional chemical tracer model driven by assimilated meteorological fields, *J. Geophys. Res.*, *106*, 12,109–12,128, 2001.

Lobert, J., W. Keen, J. Logan, and R. Yevich, Global chlorine emissions from biomass burning: Reactive chlorine emissions inventory, *J. Geophys. Res.*, *104*, 8373–8389, 1999.

Malm, W. C., J. F. Sisler, D. Huffman, R. A. Eldred, and T. A. Cahill, Spatial and seasonal trends in particle concentration and optical extinction in the United States, *J. Geophys. Res.*, *99*, 1347–1370, 1994.

Malm, W. C., M. L. Pitchford, M. Scruggs, J. F. Sisler, R. Ames, S. Copeland, K. A. Gebhart, and D. E. Day, Spatial and seasonal patterns and temporal variability of haze and its consituents in the United States, *Rep. III*, Coop. Inst. for Res., Colo. St. Univ., Fort Collins, Colo., 2000.

McKeen, S. A., G. Wotawa, D. D. Parrish, J. S. Holloway, M. P. Buhr, G. Hübler, F. C. Fehsenfeld, and J. F. Meagher, Ozone production from Canadian wildfires during June and July of 1995, *J. Geophys. Res.*, *107*(D14), 4192, doi:10.1029/2001JD000697, 2002.

Peppler, R. A., et al., ARM southern Great Plains site observations of the smoke pall associated with the 1998 Central American fires, *Bull. Am. Meteorol. Soc.*, *81*, 2563–2591, 2000.

Rogers, C. M., and K. P. Bowman, Transport of smoke from the Central American fires of 1998, *J. Geosphy. Res*, *106*, 28,357–28,368, 2001.

Seinfeld, J. H., and S. N. Pandis, *Atmospheric Chemistry and Physics: From Air Pollution to Climate Change*, John Wiley, New York, 1998.

Stohl, A., A 1-year Lagrangian "climatology" of airstreams in the Northern Hemisphere troposphere and lowermost stratosphere, *J. Geophys. Res.*, *106*, 7263–7279, 2001.

Streets, D. G., S. Gupta, S. T. Waldhoff, M. Q. Wang, T. C. Bond, and B. Yiyun, Black carbon emissions in China, *Atmos. Environ.*, *35*, 4281–4296, 2001.

Walcek, C. J., R. A. Brost, and J. S. Chang, SO_2, sulfate and HNO_3 deposition velocities computed using regional landuse and meteorological data, *Atmos. Environ.*, *20*, 949–964, 1986.

Wotawa, G., and M. Trainer, The influence of Canadian forest fires on pollutant concentrations in the United States, *Science*, *288*, 324–328, 2000.

Yevich, R., and J. A. Logan, An assesment of biofuel use and burning of agricultural waste in the developing world, *Global Biogeochem. Cycles*, *17*, doi:10.1029/2002GB001952, in press, 2003.

M. Chin, School of Earth and Atmospheric Sciences, Georgia Institute of Technology, Atlanta, Georgia, USA. (chin@rondo.gsfc.nasa.gov)

D. J. Jacob and R. J. Park, Division of Engineering and Applied Sciences and Department of Earth and Planetary Sciences, Harvard University, Cambridge, MA 02138, USA. (djacob@fas.harvard.edu; rjp@io.harvard.edu)

R. V. Martin, Harvard-Smithsonian Center for Astrophysics, Cambridge, MA, USA. (rvmartin@fas.harvard.edu)

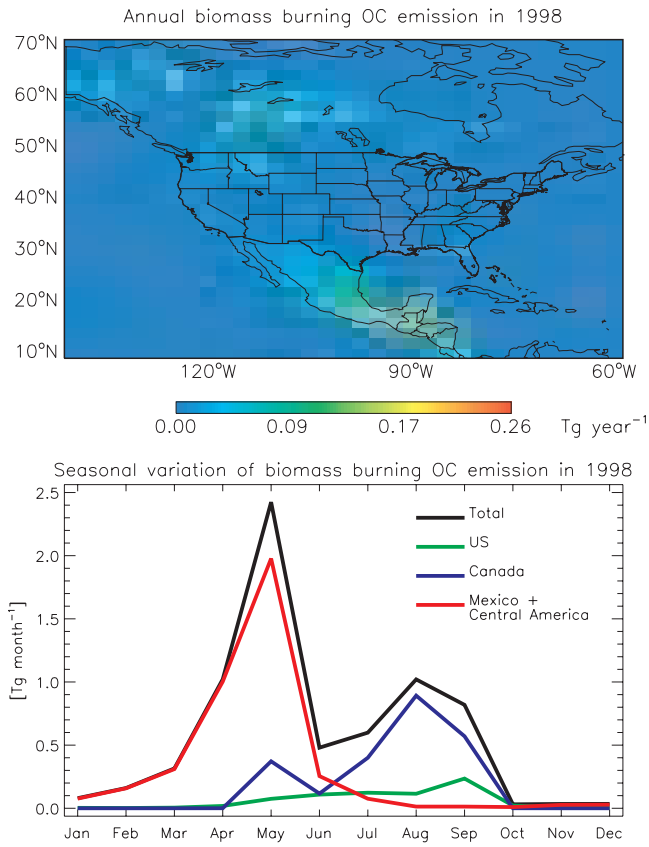

Figure 2. Annual biomass burning OC emission over North and Central America in 1998 (top) and seasonal variations for different regions (bottom).

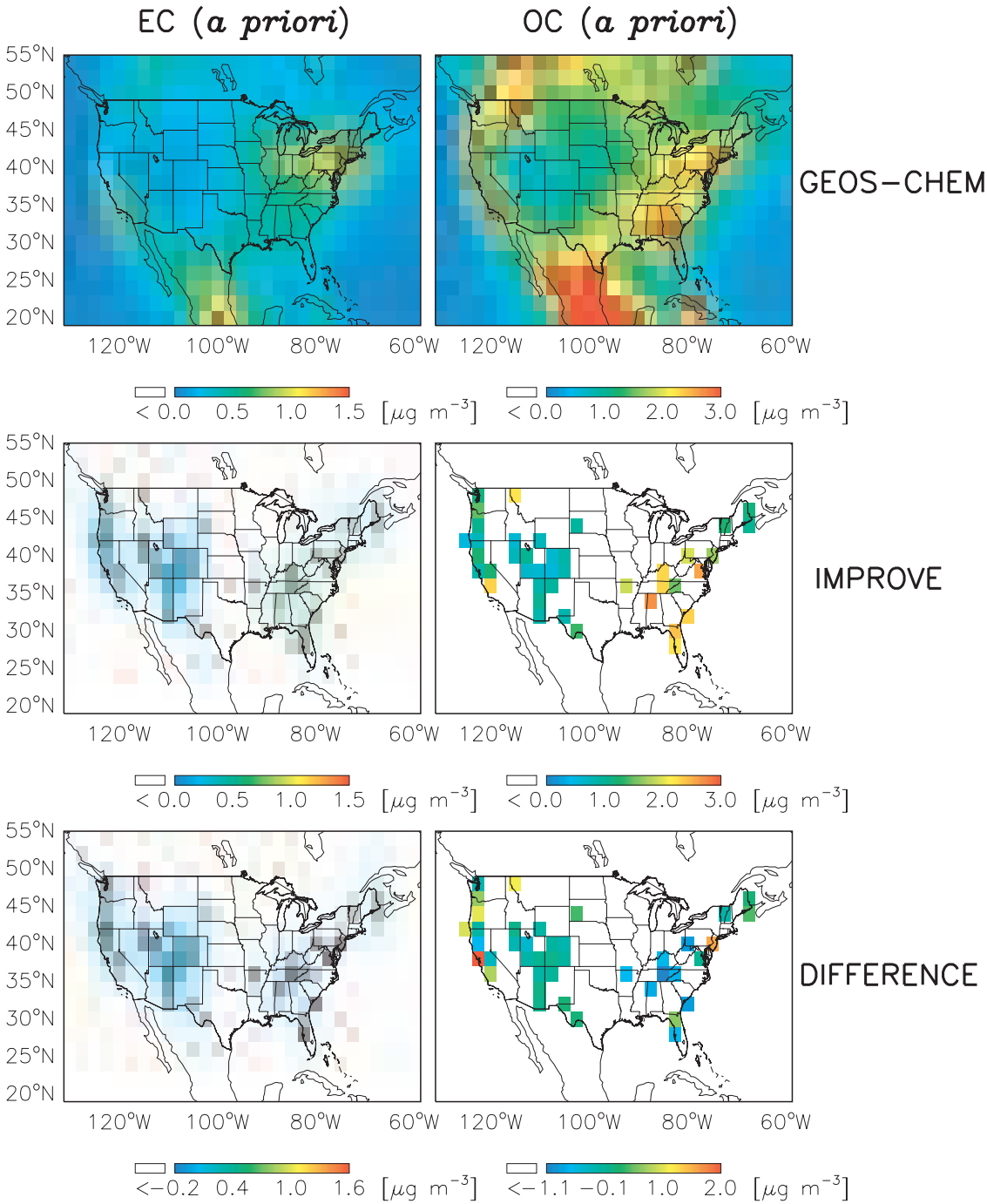

Figure 4. Annual mean concentrations of EC (left) and OC (right) in surface air over the United States in 1998. The top panels show results from the GEOS-CHEM model using a priori sources. The middle panels shows the IMPROVE observations plotted on the model 2° × 2.5° grid. The bottom panel shows the difference between the two.

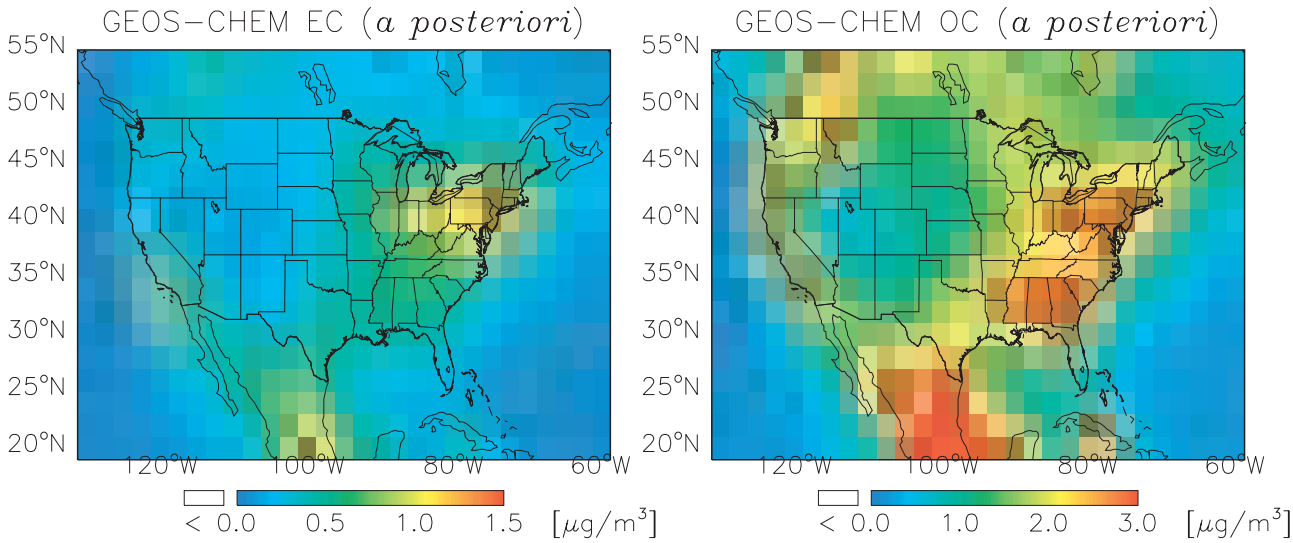

Figure 9. Annual mean concentrations of EC (left) and OC (right) in surface air over the United States in 1998 from the GEOS-CHEM model using a posteriori sources.

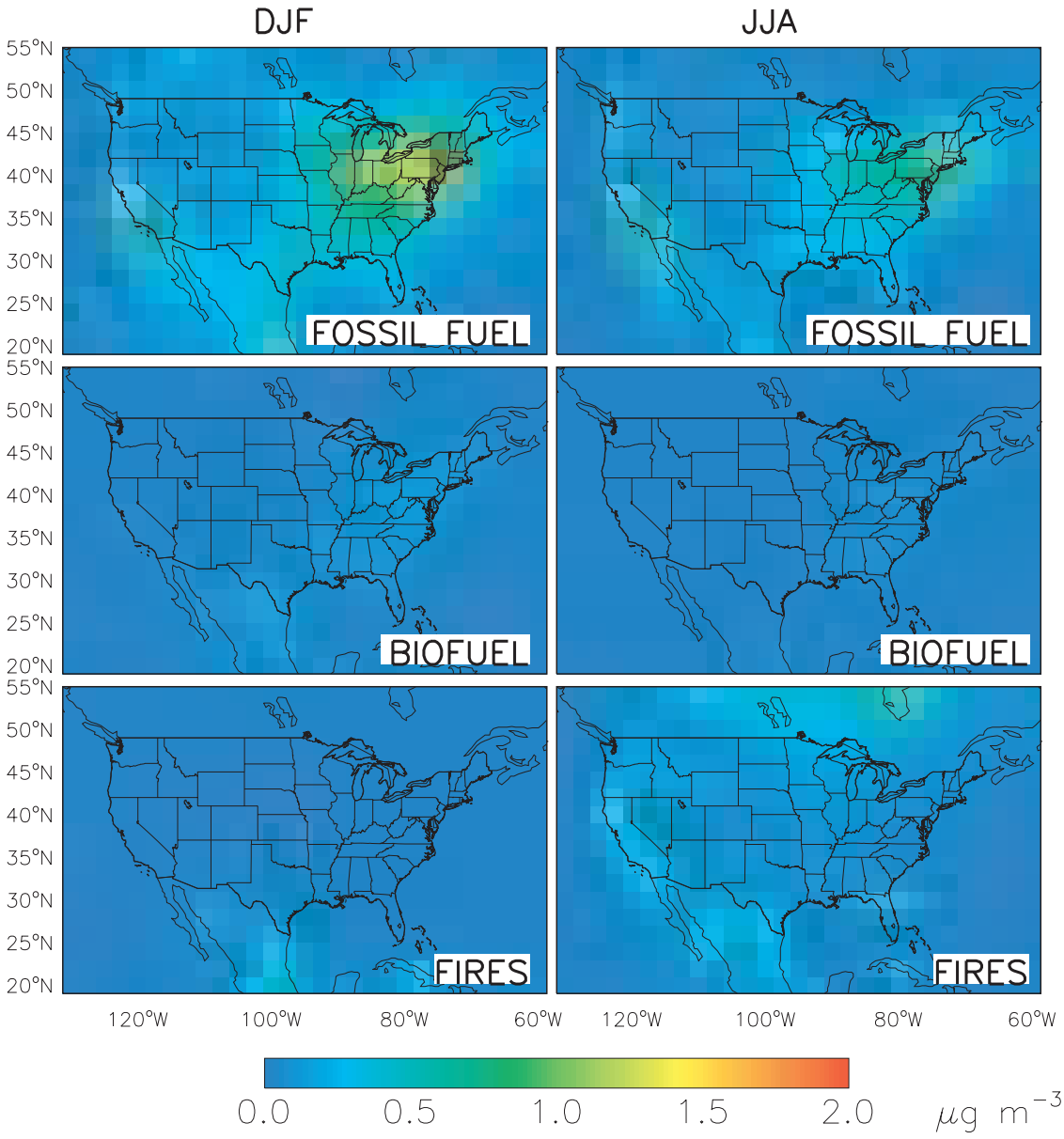

Figure 10. Contribution from different sources types to EC concentrations ($\mu g\ m^{-3}$) in surface air for DJF and JJA. Values are model results for 1998 using a posteriori sources (Table 1).

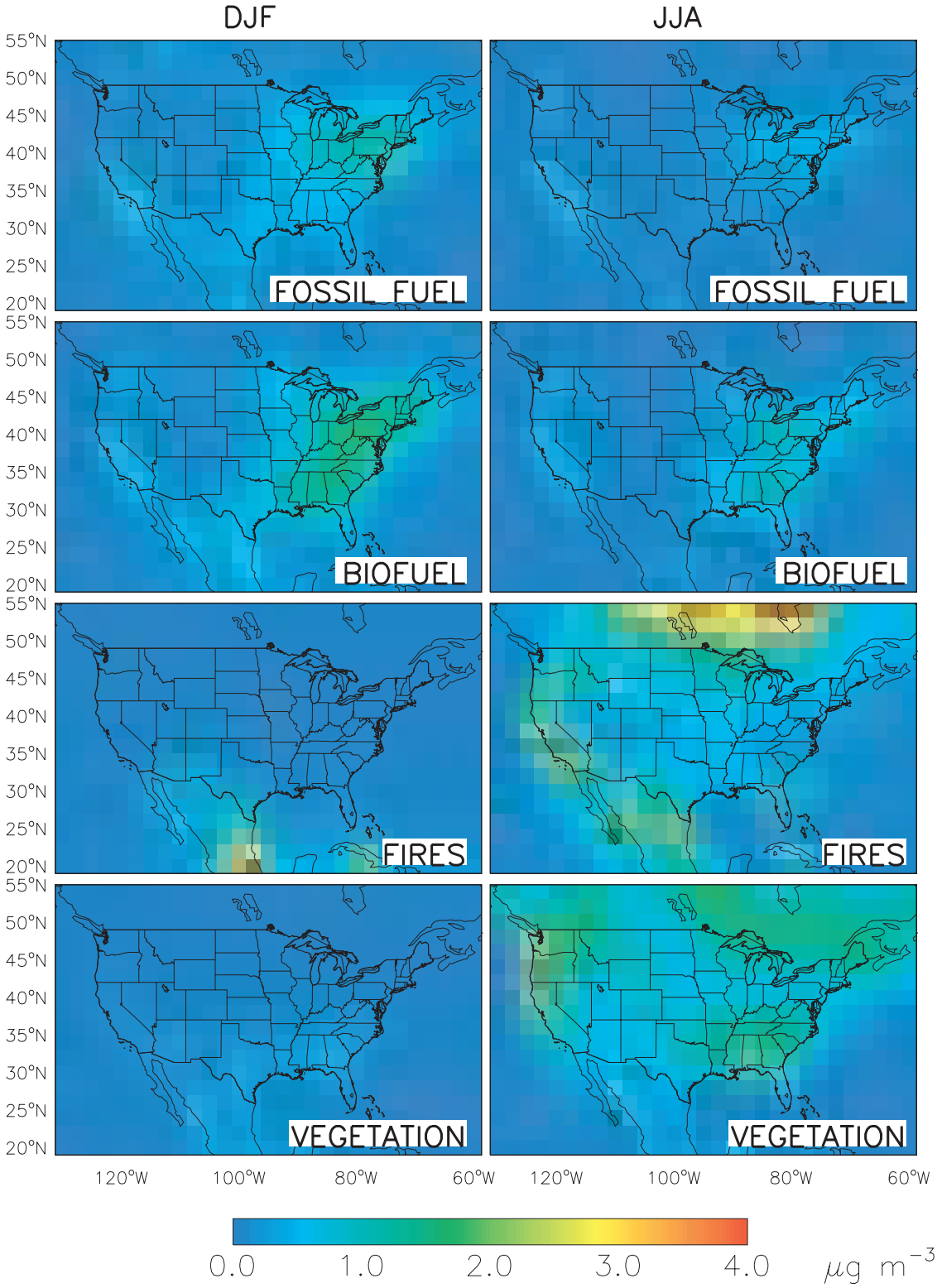

Figure 11. Same as Figure 10 but for OC.